Two Types of X-ray Spectra in Cataclysmic Variables

K. Mukai[1,2]

Code 662, NASA/Goddard Space Flight Center, Greenbelt, MD 20771, USA.

and

A. Kinkhabwala, J.R. Peterson, S.M. Kahn, F. Paerels,

Columbia Astrophysics Laboratory, Columbia University, 550 West 120th Street, New York, New York 10027, USA.

ABSTRACT

We present *Chandra* HETG spectra of seven cataclysmic variables. We find that they divide unambiguously into two distinct types. Spectra of the first type are remarkably well fit by a simple cooling flow model, which assumes only steady-state isobaric radiative cooling. The maximum temperature, $kT_{\rm max}$, and the normalization, which provides a highly precise measurement of the accretion rate, are the only free parameters of this model. Spectra of the second type are grossly inconsistent with a cooling flow model. They instead exhibit a hard continuum, and show strong H-like and He-like ion emission but little Fe L-shell emission, which is consistent with expectations for line emission from a photoionized plasma. Using a simple photoionization model, we argue that the observed line emission for these sources can be driven entirely by the hard continuum. The physical significance of these two distinct types of X-ray spectra is also explored.

Subject headings: Novae, cataclysmic variables — X-rays: binaries

1. Introduction

Cataclysmic variables (CVs) are interacting binaries in which the accreting object (the primary) is a white dwarf (see Warner 1995 for a review). X-ray emission in CVs is most

[1]Also Universities Space Research Association

[2]Also Columbia Astrophysics Laboratory, Columbia University, 550 West 120th Street, New York, New York 10027, USA

likely associated with the accretion process, which is capable of shock-heating accreted material up to high temperatures ($kT_{\rm max} \sim$ 10–50 keV). Their accretion geometry is strongly influenced by the magnetic field of the primary. Non-magnetic systems have undisrupted accretion disks that connect to the white dwarf surface via a boundary layer (Patterson & Raymond 1985). In magnetic systems, the accretion stream follows the primary's magnetic field lines, and is close to vertical when it hits the surface (see, e.g., Aizu 1973). In both cases, the emergent X-ray spectrum is expected to be the sum of emission from plasmas over a continuous temperature distribution, from the shock temperature to the white dwarf photospheric temperature.

2. Observations and Spectra

Seven CVs were observed with *Chandra* HETG by 2002 March; we have obtained these data from the archive and analyzed them using CIAO 2.2.1. The objects are four magnetic CVs of the intermediate polar (IP) class (EX Hya, V1223 Sgr, AO Psc, and GK Per), two dwarf novae (SS Cyg and U Gem), and one old nova (V603 Aql). For CVs with multiple HETG observations, we have chosen to analyze one spectrum per system (quiescent spectrum of SS Cyg, and one of two similar spectra of GK Per). Previous publications from these data exist for EX Hya (Mauche et al. 2001; Mauche 2002) and U Gem (Szkody et al. 2002).

These seven X-ray spectra divide unambiguously into two types. Spectra of the first type are well fit by a simple cooling flow model, whereas spectra of the second type are well described by a simple model of a photoionized plasma. Combined first-order ($m = \pm 1$) MEG spectra of cooling flow CVs and of photoionized CVs are shown in Figs. 1 and 2, respectively, and are discussed below in §3.1 and §3.2, respectively.

3. Spectral Analysis

3.1. Cooling Flow Spectra

The four CV spectra of EX Hya, V603 Aql, U Gem, and SS Cyg shown in Fig. 1 are strikingly similar. These spectra exhibit a smooth continuum, strong H- and He-like ion emission lines of O, Ne, Mg, Al, Si, and S, and strong emission from ions spanning the entire Fe L-shell complex (Fe XVII-Fe XXIV). In the HEG spectra (not shown), H- and He-like Fe lines are strong, while the intensity of the Fe fluorescence line varies from system to system.

The observed wide range and strengths of emission from H- and He-like ions, the level

and shape of the continuum (suggesting bremsstrahlung), and, in particular, the comparable strengths of emission across the full range of Fe L-shell ions are all consistent with expectations for a multitemperature thermal plasma with a relatively flat emission measure distribution. The flatness of this distribution is further indicative of an isobaric cooling flow, which assumes only that the gas releases all of its energy in the form of optically-thin radiation as it cools in a steady-state flow. The two main parameters of this model are the maximum temperature, $kT_{\rm max}$, and the overall normalization, which directly gives the total mass flow rate. Fits to the spectra using `mkcflow` (Mushotzky & Szymkowiak 1988) (with a uniform velocity broadening and an interstellar absorber) in `xspec` (Arnaud 1996) are shown in red in Fig. 1 with model parameters listed in Table 1. We obtain the same $kT_{\rm max}$ of 20 keV for EX Hya, V603 Aql, and U Gem, but a $kT_{\rm max}$ of 80 keV for SS Cyg, accounting for the stronger continuum in this source. The total mass flow rates listed in Table 1, which we have not scaled to the best-estimate distances to these CVs, are nonetheless entirely reasonable.

These high resolution observations unambiguously demonstrate that post-shock plasmas in some CVs are cooling flows, as originally pointed out by Fabian & Nulsen (1977) and applied to CVs by Done et al. (1995). Interestingly, the `mkcflow` model developed for clusters of galaxies can be used to fit CV spectra, while it is now known that clusters are poorly described by such a model (Peterson et al. 2001, 2002).

Our models (Fig. 1) generally predict line strengths to within a factor of two, setting the maximum level for abundance differences from our assumption (solar). Some of these discrepancies, such as in the Fe XVII line complex, are more likely due to effects arising from line opacity, density, or UV irradiation, rather than abundance (especially given the concordance of the Fe XVIII–Fe XXIV lines). We also note that He-like triplets (e.g., O VII, Ne IX, and Mg XI), whenever data quality is sufficiently high to be resolvable, show evidence for forbidden-to-intercombination line conversion through excitation of the long-lived 2 ^{3}S$_1$ level up to the 2 ^{3}P multiplet (Gabriel & Jordan 1969); both electron collisional excitation (e.g., Porquet & Dubau 2000) and photoexcitation due to UV photons from the white dwarf surface (e.g., Kahn et al. 2001) are potentially important in driving this conversion.

3.2. Photoionized Spectra

The spectra shown in Fig. 2 are noticeably different from those shown in Fig. 1, but are very similar to one another. In particular, V1223 Sgr and AO Psc both have a hard, power-law-like continuum, and strong lines from medium Z elements, but the Fe L-shell emission is limited only to Fe XVII lines, with no detectable Fe XVIII-Fe XXIV lines. This

does not indicate a low Fe abundance, since we detect strong Kα lines (H-like, He-like, and fluorescence) in the HEG spectra (not shown). GK Per has a continuum that is harder still, and shows H- and He-like ions but little Fe L-shell emission. This type of emission line spectrum is incompatible with cooling flow plasma. Instead, it resembles the expectations for photoionized plasma (Liedahl 1999; Sako et al. 2000), and the observed spectrum of the prototype Seyfert 2, NGC 1068, for which photoionization origin has been demonstrated (Kinkhabwala et al. 2002), confirming the earlier suggestion by Kallman et al. (1993).

We model these spectra with the `xspec` photoionization model `photoion`[3] (Kinkhabwala et al. 2002, 2003). We assume that the observed continuum of V1223 Sgr and AO Psc is that which drives the line emission, while a similar continuum (shown as the blue line in Fig. 2) drives the photoionization in GK Per but is obscured along our particular line of sight. We also assume the line emission is unabsorbed in all three systems. Furthermore, we assume that all lines remain completely unsaturated at all ionic column densities, due to radial velocity distribution widths of thousands of km s^{-1}. This last assumption is necessary to explain the strong resonance lines in the He-like triplets, which are not predicted by traditional photoionization models (Porquet & Dubau 2000). With these assumptions, we find that a simple model of a photoionized cone of plasma fits the data very well. We show the model fits in Fig. 2 in red (showing the absorbed continuum plus unabsorbed lines in the case of GK Per), and list the corresponding model parameters in Table 2. Included in this table are the lower limits to the accretion rates necessary to power the photoionizing continuum. These values are similar to the mass flow rates in the cooling-flow CVs.

The presence of line emission from O VII to S XVI in all spectra is consistent with a broad, relatively flat distribution in log ionization parameter, as inferred for NGC 1068 (Kinkhabwala et al. 2002), and with near solar abundances. The exception is the large nitrogen to oxygen ratio in GK Per, mirroring the unusual UV line ratios (Mauche et al. 1997), and may suggest an abundance anomaly for this system with an evolved secondary (Kraft 1964). As with the cooling flow cases, the He-like triplets again exhibit conversion of the forbidden to intercombination lines, suggesting high electron density and/or a strong, ambient UV radiation field.

4. Discussion

We have shown that a simple cooling flow model is capable of reproducing the X-ray spectra of four CVs, while a photoionization model can successfully reproduce the strikingly

[3]http://xmm.astro.columbia.edu/photoion/photoion.html

different spectra of three other CVs. The latter are all magnetic systems of the IP type, while the former is a mixture of EX Hya, an unusual IP, and non-magnetic systems. Both the fact that the X-ray spectral types almost coincide with the classification into magnetic and non-magnetic systems, and the somewhat surprising fact that this match is not exact, requires explanation.

The difference between the two X-ray spectral types may be the specific accretion rate (accretion rate per unit area). In most IPs, the magnetic field collimates the flow onto small regions (<0.2% of the white dwarf surface in XY Ari: Hellier 1997). EX Hya, however, is thought to have a much lower specific accretion rate than typical IPs, creating a tall, lower density, shock (Allan et al. 1998). The resultant top-hat geometry of the post-shock region will allow the cooling flow X-rays to escape the post-shock region from the side without having to travel through the pre-shock flow. The boundary layer in non-magnetic CVs probably cover a much larger area than the spot on XY Ari. This would lead to a specific accretion rate that is always low enough to allow the X-rays to escape freely. In this view, all CVs with low specific accretion rate (all non-magnetic systems, as well as some magnetic systems) should show a cooling flow-like X-ray spectrum.

On the other hand, typical IPs such as V1223 Sgr and AO Psc probably have a high specific accretion rate, leading to a pillbox geometry which does not allow the cooling flow spectrum to escape freely. If true, these systems are also powered by the cooling flow continuum (compare the measured $\dot{M}$ in Table 1 with the inferred values in Table 2), which is differentially absorbed. The apparent lack of the cooling-flow line emission may be due to a larger optical depth along the line of sight to the post-shock region than to the photoionized plasma, allowing the latter to dominate the observed spectrum. Although a model of a multitemperature bremsstrahlung continuum with multiple partial covering absorbers can reproduce the observed continuum shape, this does beg the question of why we observe such highly similar hard continua in V1223 Sgr and AO Psc. If this cannot be explained without an excessive degree of fine-tuning, we may be forced to explore an alternative origin of the ionizing continuum.

Evidence that the photoionized emission arises from pre-shock flow comes from the inferred large radial velocity distribution, which is present only in the near free-fall pre-shock flow. Further evidence may come from GK Per. The shorter-wavelength, higher-ionization line strengths are significantly weaker in this source than in the other two. If, for GK Per, we discard the assumption that the line emission is unabsorbed, and instead assume that its line emission spectrum is intrinsically similar to that of V1223 Sgr and AO Psc, then GK Per must be differentially obscured, with obscuration increasing with ionization parameter all the way down to the photoionizing continuum. This favors a spatially-stratified ionization

model, which should arise naturally in an accretion flow, rather than the intrinsic density distribution that leads to the range of ionization in NGC 1068 (Brinkman et al. 2002).

The existence of two types of X-ray spectra in the HETG range among accreting CVs is beyond doubt. However, our interpretation is admittedly somewhat tentative, and that other system parameters (such as the primary mass and the inclination angle) may also play an important role in shaping the observed X-ray spectra. It is also possible that there are yet other types of CV X-ray spectrum in the HETG range, such as the wind-scattered X-rays seen at longer wavelengths (see, e.g., Kuulkers et al. 2002). Further high resolution X-ray spectroscopy of a larger sample of CVs, and more detailed analyses of the existing spectra, should be helpful in clarifying both points.

We thank Ming Feng Gu for previous extensive help with his atomic code FAC, and Coel Hellier and Chris Mauche for useful discussion. The Columbia University team is supported by NASA. AK acknowledges additional support from a NASA GSRP fellowship.

REFERENCES

Aizu, K. 1973, Prog. Theor. Phys., 49, 1184

Allan, A., Hellier, C., & Beardmore, A.P. 1998, MNRAS, 295, 167

Arnaud, K.A., in "Astronomical Data Analysis Systems V," eds. G.H. Jacoby & J. Barnes (San Francisco: ASP), 17

Brinkman, A.C., Kaastra, J.S., van der Meer, R.L.J., Kinkhabwala, A., Behar, E., Paerels, F.B.S., Kahn, S.M., Sako, M. 2002, A&A, 396, 761

Done, C., Osborne, J.P., & Beardmore, A.P. 1995, MNRAS, 276, 483

Fabian, A.C., Nulsen, P.E.J. 1977, MNRAS, 180, 479

Gabriel, A.H., & Jordan, C. 1969, MNRAS, 145, 241

Hellier, C 1997, MNRAS, 291, 71

Kahn, S.M., Leutenegger, M.A., Cottam, J., Rauw, G., Vreux, J.-M., den Boggende, A.J.F., Mewe, R., & Güdel, M. 2001, A&A, 365, L312

Kallman, T.R., et al. 1993, ApJ, 411, 869

Kinkhabwala, A., Sako, M., Behar, E., Kahn, S.M., Paerels, F.B.S., Brinkman, A.C., Kaastra, J.S., Gu, M.F., & Liedahl, D.A. 2002, ApJ, 575, 732

Kinkhabwala, A., Behar, E., Sako, M., Gu, M.F., Kahn, S.M., & Paerels, F.B.S. 2003, in preparation

Kraft, R.P. 1964, ApJ, 139, 457

Kuulkers, E., Knigge, C., Steeghs, D., Wheatley, P.J., & Long, K.S. 2002, in "The Physics of Cataclysmic Variables and Related Objects," eds. B.T. Gänsicke, K. Beuermann & K. Reinsch (San Francisco: Astronomical Society of the Pacific), 443

Liedahl, D.A. 1999, in "X-Ray Spectroscopy in Astrophysics," eds. J. van Paradijs & J. A. M. Bleeker (Berlin: Springer)

Mauche, C.W. 2002, in "The Physics of Cataclysmic Variables and Related Objects," eds. B.T. Gänsicke, K. Beuermann & K. Reinsch (San Francisco: Astronomical Society of the Pacific), 113

Mauche, C.W., Lee, Y.P. & Kallman, T.R. 1997, ApJ, 477, 832

Mauche, C.W., Liedahl, D.A., & Fournier, K.B. 2001, ApJ, 560, 992

Mushotzky, R.F., & Szymkowiak, A.E. 1988, in "Cooling Flows in Clusters and Galaxies," ed. A.C. Fabian, Dordrecht, Netherlands, Kluwer Academic Publishers, 53

Patterson, J., & Raymond, J.C. 1985, ApJ, 292, 535

Peterson, J.R., Paerels, F.B.S., Kaastra, J.S., Arnaud, M., Reiprich, T. H., Fabian, A. C., Mushotzky, R. F., Jernigan, J. G., & Sakelliou, I. 2001, A&A, 365, L104

Peterson, J.R., Kahn, S.M., Paerels, F.B.S., Kaastra, J.S., Tamura, T., Bleeker, J.A.M., Ferrigno, C., & Jernigan, J.G. 2002, ApJ, submitted (astro-ph/0210662)

Porquet, D., & Dubau, J. 2000, A&AS, 143, 495

Sako, M., Kahn, S.M., Paerels, F.B.S., & Liedahl, D.A. 2000, ApJ, 543, L115

Szkody, P., Nishikida, K., Raymond, J.C., Seth, A., Hoard, D.W., Long, K.S., & Sion, E.M. 2002, ApJ, 574, 942

Warner 1995, *Cataclysmic Variables* (Cambridge: Cambridge Univ. Press)

AAS LaTeX macros v5.0.

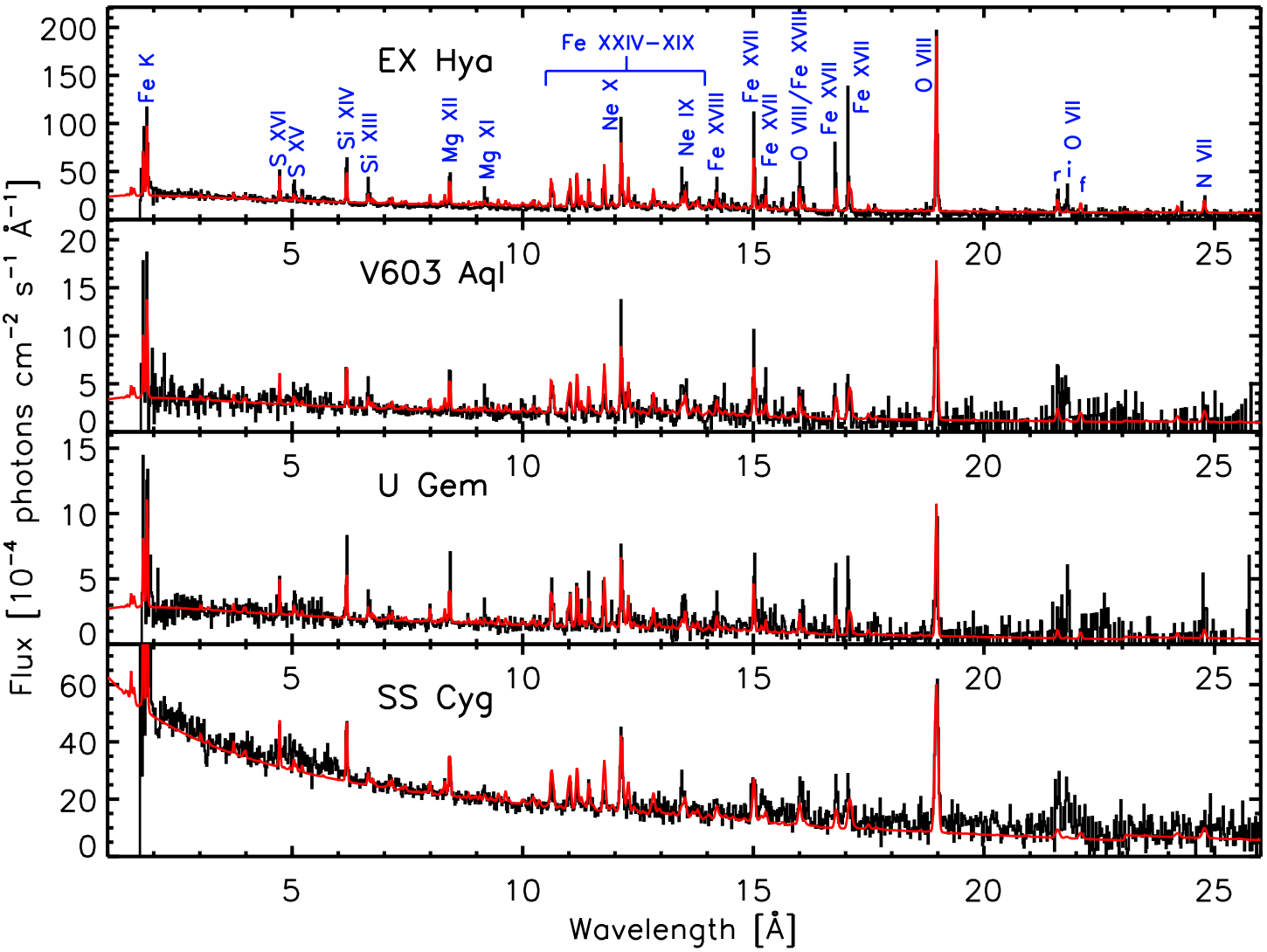

Fig. 1.— *Chandra* HETG spectra (MEG, $m = \pm 1$ orders) of 4 CVs that exhibit cooling flow spectra. Data are shown in black with the corresponding cooling flow model shown in red.

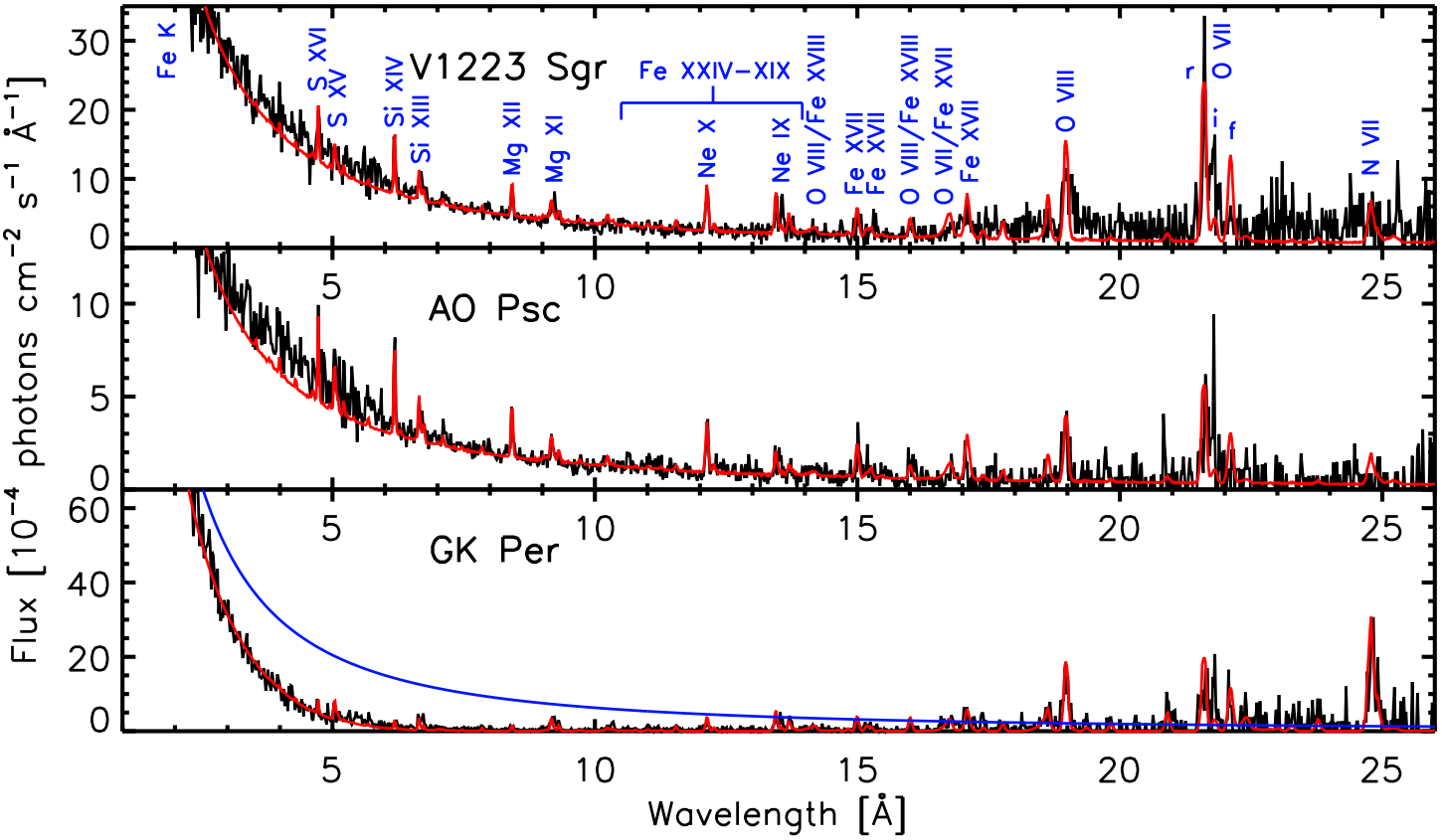

Fig. 2.— *Chandra* HETG spectra (MEG, $m = \pm 1$ orders) of 3 CVs that exhibit photoionized models. Data are shown in black with the corresponding photoionization model shown in red. The blue line in the bottom panel shows the inferred intrinsic continuum for GK Per.

Table 1. Cooling Flow CVs.

Model Parameters	EX Hya 1706[a]	V603 Aql 1901[a]	U Gem 647[a]	SS Cyg 3454[a]
$N_{\rm H}$ [cm^{-2}]	2e20	2e20	1e21	7e20
σ_v [km s^{-1}][b]	200	400	300	550
$kT_{\rm max}$ [keV]	20	20	20	80
$\dot{M}\, d_{100}^{-2}$ [c]	3.9e-11	5.6e-12	4.4e-12	2.6e-11

[a]ObsID.

[b]Observed line width, assuming a constant velocity broadening for all lines.

[c]Mass flow rate for an assumed distance of 100 pc in $M_\odot$ yr^{-1}.

Table 2. Photoionized CVs.

Model Parameters	V1223 Sgr 649[a]	AO Psc 1898[a]	GK Per 3454[a]
f [b]	0.5	0.5	0.5
$N_{\rm H}^{\rm intrinsic}$ [cm^{-2}] [c]	0	0	7e22
σ_v [km s^{-1}][d]	600	600	600
$L_X\, d_{100}^{-2}$ [e]	1.6e32	6e31	2.9e32
$\dot{M}\, d_{100}^{-2}$ [f]	>9.4e-12	>3.5e-12	>1.7e-11
Ionic Column Densities [cm^{-2}]			
N VI	8e17	5e17	2e18
O VII	2.5e18	1.3e18	1.2e18
O VIII	1.7e18	1e18	1.2e18
Ne IX	4e17	2e17	2e17
Ne X	5e17	5e17	1.5e17
Mg XI	1.7e17	2e17	1e17
Mg XII	3.2e17	4.7e17	5e16
Si XIII	1.7e17	2.5e17	7e16
Si XIV	5e17	7e17	7e16
S XV	1.5e17	2.5e17	1e17
S XVI	4e17	6e17	1e17
Fe XVII	2e17	2e17	1e17

[a]ObsID.

[b]Covering fraction $f = \Omega/4\pi$ for cone geometry.

[c]Required obscuration of inferred continuum for GK Per.

[d]Observed line width, assuming a constant velocity broadening for all lines.

[e]Bolometric power-law $L(E) \propto E^{-0.3}$ (13.6 eV$< E <$ 10 keV) luminosity for an assumed distance of 100 pc in ergs s^{-1}.

[f]Minimum accretion rate for an assumed distance of 100 pc in M$_\odot$ yr^{-1}.